A Facile Methodology for the Production of In Situ Inorganic Nanowire Hydrogels/Aerogels

Citation: Jung, Sung Mi et al. "A Facile Methodology for the Production of In Situ Inorganic Nanowire Hydrogels/Aerogels." Nano Letters 14, 4 (April 2014): 1810–1817 © 2014 American Chemical Society

As Published: http://dx.doi.org/10.1021/nl404392j

Publisher: American Chemical Society (ACS)

Persistent URL: http://hdl.handle.net/1721.1/111112

Version: Author's final manuscript: final author's manuscript post peer review, without publisher's formatting or copy editing

NANO LETTERS

Letter

pubs.acs.org/NanoLett

A Facile Methodology for the Production of In Situ Inorganic Nanowire Hydrogels/Aerogels

Sung Mi Jung,[†,⊥] Hyun Young Jung,[‡,⊥] Wenjing Fang,[†] Mildred S. Dresselhaus,[†,§] and Jing Kong*[,†]

[†]Department of Electrical Engineering and Computer Sciences, Massachusetts Institute of Technology, Cambridge, Massachusetts 02139, United States

[‡]Department of Mechanical and Industrial Engineering, Northeastern University, Boston, Massachusetts 02115, United States

[§]Department of Physics, Massachusetts Institute of Technology, Cambridge, Massachusetts 02139, United States

Supporting Information

ABSTRACT: Creating inorganic nanowire hydrogels/aerogels using various materials and inexpensive means remains an outstanding challenge despite their importance for many applications. Here, we present a facile methodology to enable highly porous inorganic nanowire hydrogel/aerogel production on a large scale and at low cost. The hydrogels/aerogels are obtained from in situ hydrothermal synthesis of one-dimensional (1D) nanowires that directly form a cross-linking network during the synthesis process. Such a method not only offers great simplicity but also allows the interconnecting nanowires to have much longer length. The longer length offers aerogels with remarkable porosity and surface area extremely low densities (as low as 2.9 mg/cm^3), are mechanically robust, and can have superelasticity by tuning the synthesis conditions. The nanowires in the hydrogels/aerogels serve both as structural support and active sites, for example, for catalysis or absorption. In this work, we have found that the as-grown hydrogels can be used directly as water filters to remove pollutants such as heavy metal ions and toxic organic contents. Our studies indicate that this method for nanowire hydrogels/aerogels production is not only economical but greatly augmented their applications in environmental, catalysis, sensing, absorption, energy storage, and beyond.

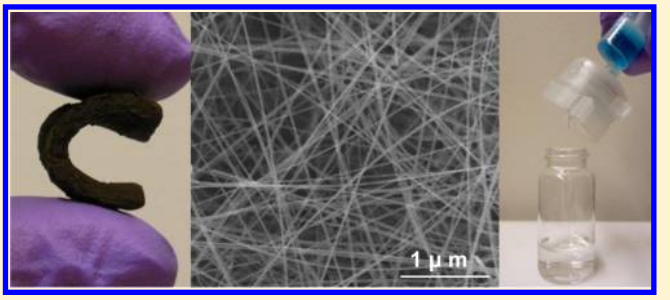

KEYWORDS: *Inorganic nanowires, hydrogels, aerogels, superelasticity, water purification filters*

Porous inorganic nanowire hydrogels/aerogels are highly attractive in applications for energy generation and storage, sensing, catalytic conversion, selective absorption and removal, or thermal insulation, and so forth.[1−4] General syntheses of the inorganic nanowire aerogels have been demonstrated with template-assisted deposition followed by a template removal step such as metal electrodeposition onto a polymer template,[5] or atomic layer deposition of a metal oxide onto nanocellulose[6] or a copolymer[7] template. However, these methods are complicated and are limited in terms of porosity[8] without collapsing of the three-dimensional (3D) network during the template removal process. Because the pore geometry and pore size play a critical role in the properties and performance of these porous materials,[9] this hampers their utilization for various applications.

Previously, we demonstrated that highly porous inorganic nanowire hydrogels/aerogels can be obtained by assembling the nanowires into a cross-linking network from their colloidal suspensions at the transition from semidilute to isotropic concentrated regimes without using templates or supporting materials.[10] The synthesized nanowires were initially dispersed with/without surfactant in ethanol using ultrasonication at a dilute concentration, and then the suspension was transformed into a nanowire gel by evaporating the solvent to reach the gel formation concentration ($\varphi_{gel} = a_r^{-1}$, where a_r is the nanowire aspect ratio, $a_r = L/d$, and L is the nanowire length and d is the diameter).[10] For this method, in the case of brittle nanowires the dispersion process results in shorter lengths and lower aspect ratios of the nanowires, which also limits the porosity of the nanowire networks.

In this work, we have come up with a much improved method to obtain porous nanowire hydrogels/aerogels directly from hydrothermal synthesis. Basically, the hydrothermal method grows the nanotubes/nanowires at elevated temperatures and under pressures in aqueous solutions[11,12] and the resulting material has been used to make nanowire blocks[13] or nanowire membranes[14−21] with limited surface area and porosity. Here, we used this method to directly produce high surface area and highly porous inorganic nanowire hydrogels/aerogels based on the principle of the gel formation in our previous work.[10] Once the concentration reaches the gel formation concentration, a nanowire gel forms in situ inside the hydrothermal vessel. The as-grown nanotube/nanowires can

Received: November 26, 2013
Revised: March 4, 2014

dx.doi.org/10.1021/nl404392j | *Nano Lett.* XXXX, XXX, XXX−XXX

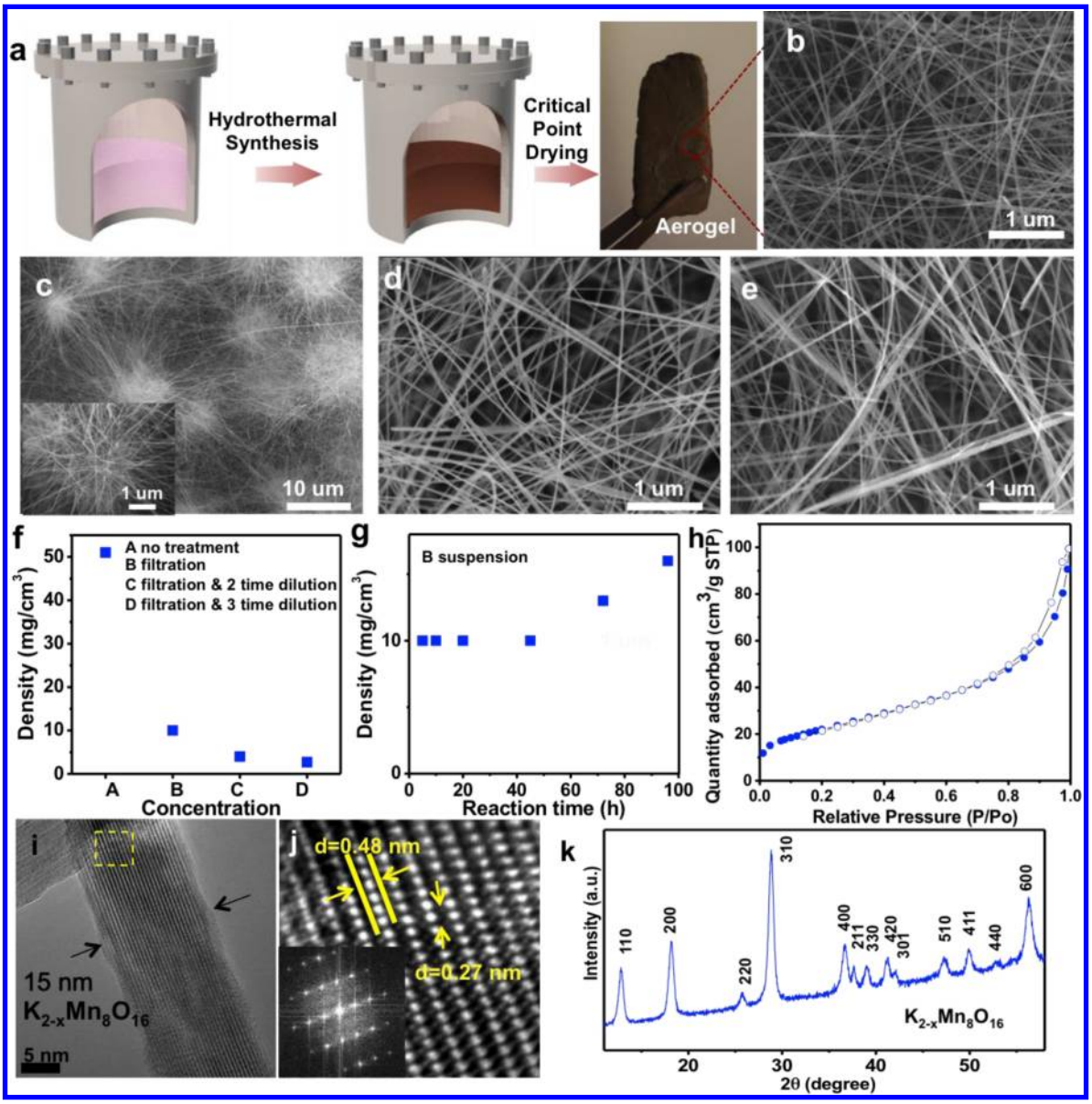

Figure 1. Structures of cryptomelane-type manganese oxide nanowire hydrogel/aerogel. (a) The inorganic nanowire hydrogel/aerogel production process. (b) SEM image of 3D network structures of cryptomelane-type manganese oxide ($K_{2-x}Mn_8O_{16}$) nanowire aerogel from suspension C with growth time of 48 h. (A, precursor suspensions without any treatment; B, filtration of A with a 0.8 μm syringe filter; C, 2-fold dilutions of B; D, 3-fold dilutions of the suspension after filtration of A with a 0.2 μm syringe filter). (c–e) SEM image of 3D network structures of the nanowire aerogel from suspension B with growth times of 5, 45, and 96 h. (f) Densities of the nanowire aerogels versus concentration of the initial suspension with a growth time of 45–48 h. (g) Densities of the nanowire aerogels versus reaction times for suspension B. (h) N_2 adsorption and desorption isotherm for the ultrafine porous aerogel with high surface areas of 80 $m^2\ g^{-1}$. (i,j) (i) TEM images of the nanowire and the SAED patterns generated by FFT from (j) (under left inset). (k) The XRD diffraction of $K_{2-x}Mn_8O_{16}$ nanowire aerogels (cryptomelane-Q type, PDF2 #42-1348; a = 9.766 Å, c = 2.842 Å).

maintain much longer lengths (hundreds of micrometers) in the network, which gives rise to much lower density, higher porosity, higher surface area, and remarkable mechanical properties for the nanowire networks. The process here is much simpler and enables large-scale production at a much lower cost when compared to our previous method.[10] Furthermore, by tuning the initial composition and concentration of the reaction precursor and the growth time for the synthesis process itself, hydrogel/aerogel networks with different diameter nanowires, different porosities, and density distributions can be obtained to suit different needs of specific applications.

Figure 1a shows the inorganic nanowire hydrogel/aerogel production process: (i) the preparation of a well-dispersed precursor suspension, (ii) the in situ nanowire hydrogel formation via hydrothermal synthesis, and (iii) the supercritical drying of the gel to form an aerogel. The ultralight and highly porous hydrogel/aerogel structures were obtained by controlling the hydrothermal synthesis conditions. There are two key elements in our method: first is the homogeneous precursor suspension at the proper precursor concentration to prevent nonuniform bundling or aggregation of nanowires; second is the proper reaction time to get an ultralong but individual nanowire network without nanowire agglomeration. These lead

dx.doi.org/10.1021/nl404392j | Nano Lett. XXXX, XXX, XXX–XXX

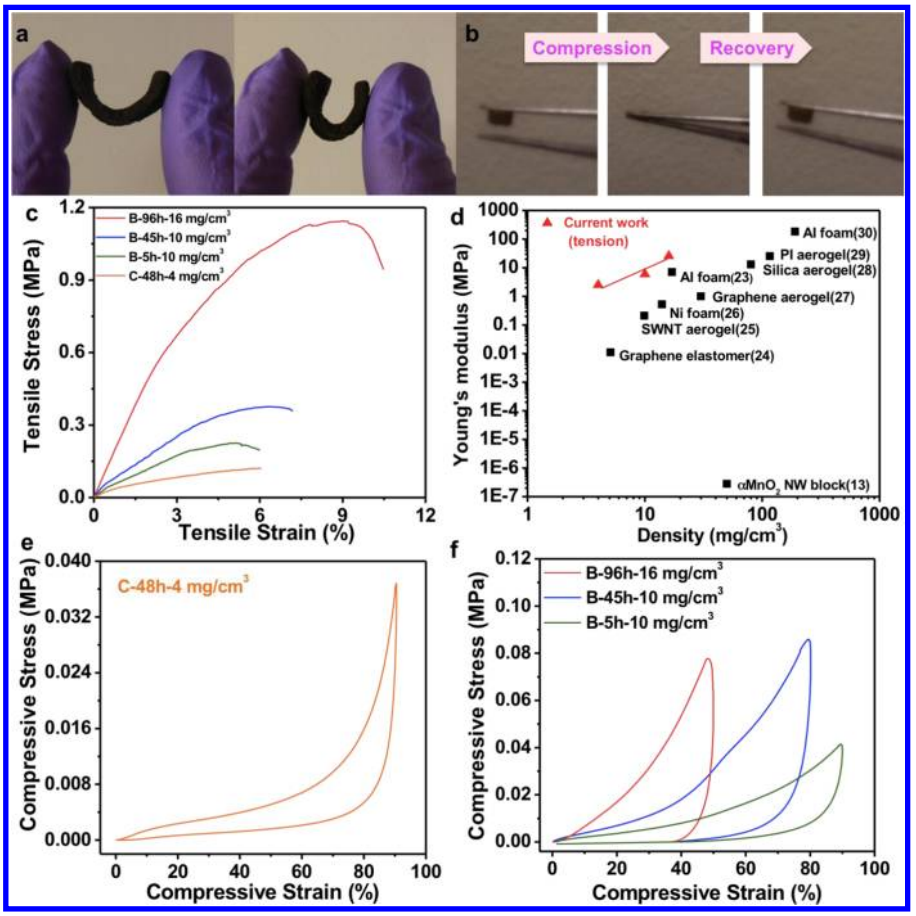

Figure 2. Mechanical properties of cryptomelane nanowire aerogels. (a,b) The aerogels with flexible, bendable, and superelastic properties. (c) Tensile test for the aerogels with different densities of 16 mg/cm^3 (B-96h-16 mg/cm^3), 10 mg/cm^3 (B-45h- 10 mg/cm^3, B-5h-10 mg/cm^3), and 4 mg/cm^3 (C-48h-4 mg/cm^3). (d) The relationship between Young's modulus and density of cryptomelane nanowire aerogels, together with data from the literature as comparison. (e,f) Compressive stress/strain tests for the aerogels with the different densities.

to a high surface area and remarkable mechanical properties for the networks, as will be shown in the following.

We produced cryptomelane manganese oxide ($K_{2-x}Mn_8O_{16}$) nanowire hydrogels/aerogels using this method. First of all, because the formation of uniform and monodispersed nanostructures requires precise control over the nucleation and growth processes,[15] the $K_{2-x}Mn_8O_{16}$ precursor suspension ($MnSO_4$, K_2SO_4, and $K_2S_2O_8$) is initially prepared by ultrasonication at room temperature and filtered with a syringe filter to get rid of undissolved precipitates caused by low solubility of potassium persulfate. After that, the suspension is transferred to a Teflon vessel and the sealed vessel is heated in an oven at 525 K for 10 min to 96 h of reaction time. During the hydrothermal reaction, the $K_{2-x}Mn_8O_{16}$ nanowires grow out from the suspension and as their length and concentration increase, they start to interconnect with each other. As time goes on, the nanowires are self-assembled into an interconnected nanowire 3D network and a nanowire hydrogel forms after a reaction time of 5 h. The in situ nanowire hydrogel networks formed at different reaction times are washed with excess DI water several times and subsequently the resultant hydrogels are supercritically dried into aerogels to retain the original gel volume.

For ultrafine and highly porous in situ 3D networks, we tuned the porosity of the aerogel via variation of the initial concentration of the precursor suspension (see Methods; A, precursor suspensions as used in our previous work[10] and ref 16 without any treatment; B, filtration of A with a 0.8 μm syringe filter; C, 2-fold dilutions of B; D, 3-fold dilutions of the suspension after filtration of A with a 0.2 μm syringe filter). The resultant aerogels obtained from B, C, and D (Figure 1d,b, Supporting Information S1a) show high porosity and high surface area due to the ultrafine nanowire network without bundles, while the aerogel obtained from A shows low porosity caused by aggregated nanowire network (Supporting Information Figure S1b). As the concentration decreases via dilution and filtration, the porosity increases and the density decreases. Especially, the aerogel from D has an extremely low density of 2.9 mg/cm^3 that is 17 times lower than the one of the previously reported MnO_2 nanowire block[13] and only slightly higher than an air density of 1.2 mg/cm^3 (Figure 1f). As we have found previously, the nanowire gel formation concentration depends on the aspect ratio of the nanowires.[10] In the present work, since the in situ nanowire gel was obtained directly from hydrothermal synthesis without any dispersion of the nanowires, ultralong nanowires with lengths up to several hundred micrometers remain in the gel network, giving rise to a very high aspect ratio. Therefore, the in situ gel could form at a much lower concentration and the resulting aerogel has a very low density.

Figure 1c–e shows the SEM images of the cryptomelane manganese oxide nanowire aerogels from in situ synthesis obtained with the same starting concentration (concentration B) with reaction times of 5, 45, and 96 h, respectively, where

dx.doi.org/10.1021/nl404392j | Nano Lett. XXXX, XXX, XXX–XXX

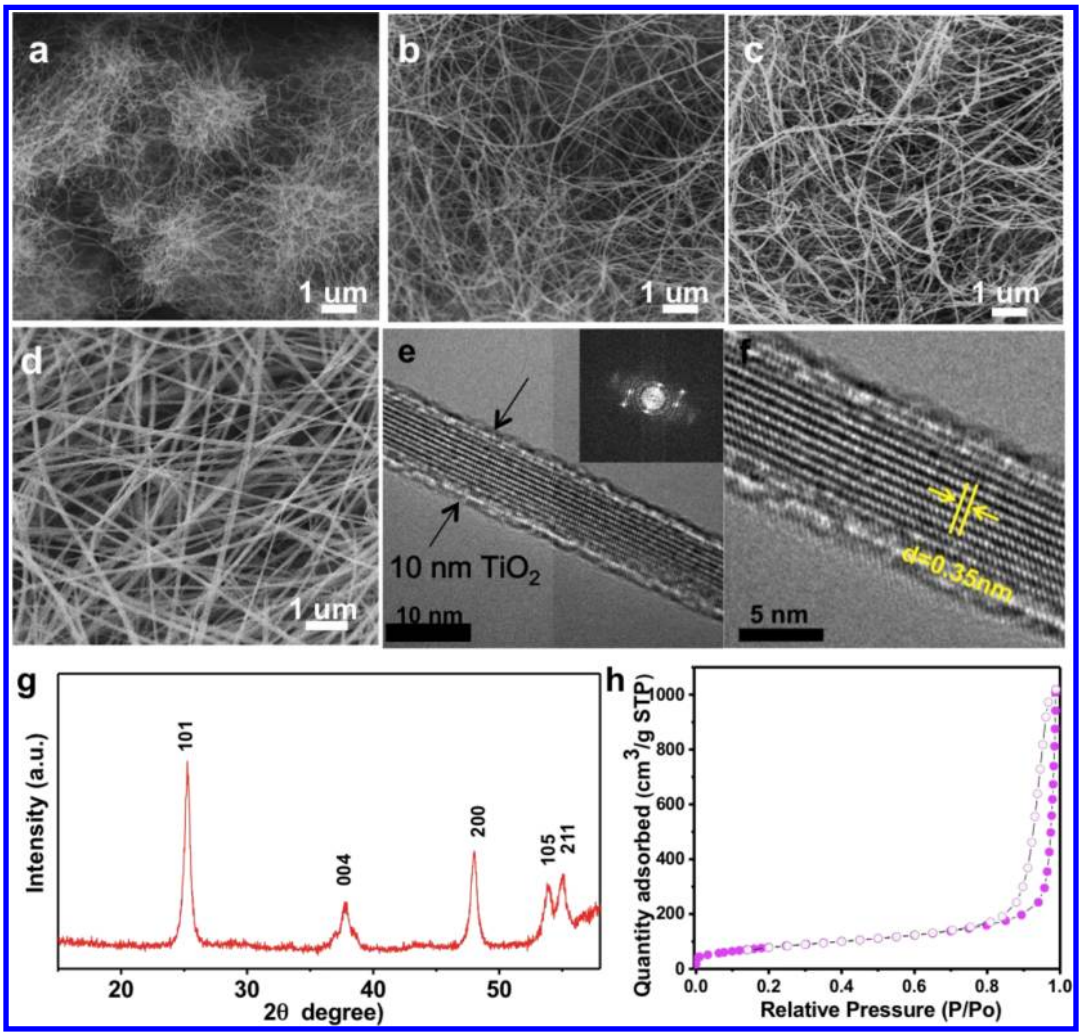

Figure 3. The characterization of structures of TiO_2 nanowire aerogels. (a–c) SEM images of TiO_2 nanowire aerogels with 5–10 nm obtained with different reaction times of 4, 16, and 48 h, respectively. (d) SEM images of TiO_2 nanowire aerogels with 50–60 nm at reaction time of 72 h. (e,f) TEM image of a highly crystalline structure of the TiO_2 nanowire with a *d*-spacing of 0.35 nm, corresponding to the spacing between (1 0 1) planes of the anatase TiO_2 phase. Inset: the SAED pattern generated by FFT from (e). (g) XRD pattern in accordance with anatase TiO_2 with crystalline cell constants a = 3.7806 Å, c = 9.4977 Å, which are basically in agreement with the reported values.[21,31] (see Supporting Information Figure S2). (h) N_2 adsorption and desorption isotherm of the sample in (b), and the surface area is found to be 292 m^2 g^{-1}).

highly porous nanowire networks are seen with pore sizes in the range of a few hundred nanometers to a few micrometers. We chose concentration B to observe the change of the network and density as a function of the reaction time. At the beginning of the reaction, small islands of nanowires could be observed in the suspension but no hydrogels could be formed. As time goes on, the islands become bigger and start to interlink with each other, and hydrogels form with the same volume as the starting suspension. Figure 1c shows the SEM of the resulting aerogel obtained with a reaction time of 5 h, where a chestnut-bur-like nanowire network can be seen. On the other hand, longer reaction time of 45 and 96 h show cross-aligned ultralong nanowire network (Figure 1d,e, respectively). Very interestingly, the densities of the nanowire networks obtained from a reaction time between 5 and 45 h gave a constant value of 10 mg/cm^3 (Figure 1g, their hydrogels have the same volume after the reaction), which suggests that between 5h and 45 h, rearrangement of the nanowires within the network occurs. (The exact mechanism is unknown yet. One possibility could be that some nanowires redissolve while others grow out, so overall the density is constant.) When the reaction time is longer than 45 h, the volume of the hydrogel (and the resulting aerogel) shrinks, giving rise to an increase in density (Figure 1g). This can be seen in the SEM of Figure 1e at an excessive reaction time of 96 h; here, some nanowire bundles in the network can be observed, possibly due to the van der Waals forces between the nanowires, resulting in a network with decreased porosity and increased density (16 mg/cm^3) and 45% shrunk in volume (Figure 1g).

The crystallinity of the synthesized nanowires were further characterized by high-resolution transmission electron microscopy (HRTEM), X-ray diffraction (XRD), and selected-area electron pattern (SAED) (Figure 1i–k). High-crystalline cryptomelane nanowires were consistently grown independent of the variations in synthesis conditions. The surface area of the sample in Figure 1d was characterized by the Brunauer–Ennett–Teller (BET) method to be 80 m^2 g^{-1} (Figure 1h), twice larger than the nanowire membranes previously reported.[16] If all the nanowires within the network are individual without bundling, it can be derived that the surface area of such aerogel should be $4/dD$, where d is the nanowire diameter and D is the density of cryptomelane. Using an

dx.doi.org/10.1021/nl404392j | Nano Lett. XXXX, XXX, XXX–XXX

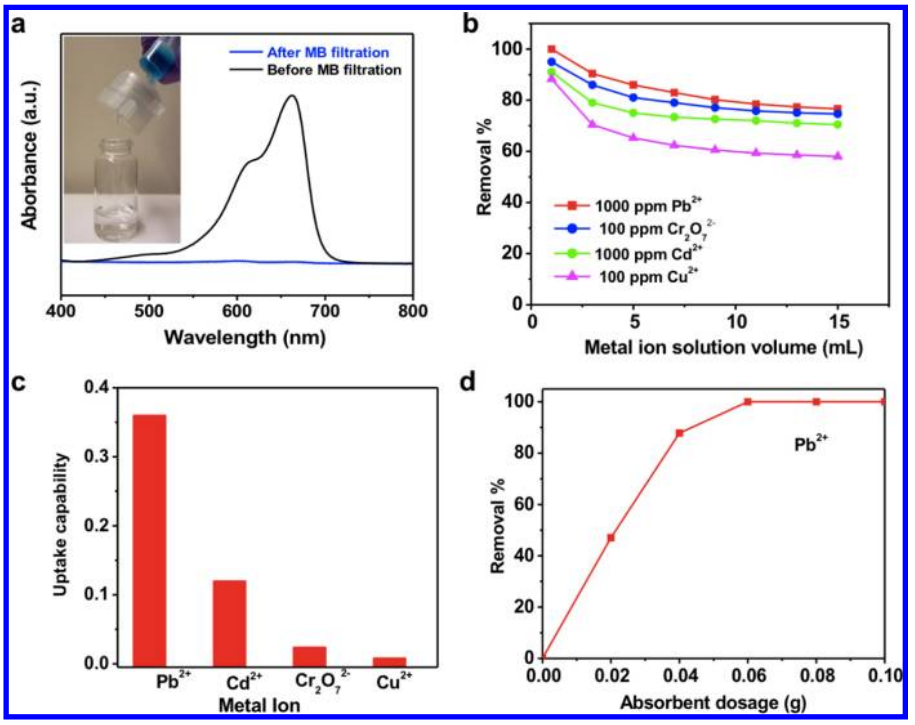

Figure 4. Water purification filters of the cryptomelane nanowire hydrogel for the removal of organic dyes and toxic heavy metal ions. (a) UV−vis-NIR spectrum before and after filtration of 0.1 wt % MB; the inset shows that an optical image of the blue solution with MB becomes clear after filtration with the cryptomelane nanowire hydrogel filter. (b) The performance of cryptomelane nanowire hydrogels (16 mg/cm^3) as water filters for the removal of heavy metal ions: 1000 ppm Pb^{2+}, 1000 ppm of Cd^{2+}, 100 ppm of $Cr_2O_7^{2-}$, or 100 ppm of Cu^{2+} in which the initial uptake capacity of Pb^{2+}, Cd^{2+}, $Cr_2O_7^{2-}$, or Cu^{2+} is 100, 91, 95, or 88.3%, respectively, and the uptake is saturated at 78, 70, 75, 59%, respectively. (c) The maximum uptake capabilities determined by the filtering experiment. (d) The absorption test using different absorbent dosages of 0.02, 0.04, 0.06, 0.08, and 0.1 g cryptomelane nanowire hydrogels, showing extremely high removal of 47, 87.8, 100, 100, and 100%, respectively. The uptake capability determined by the absorption test for Pb^{2+} is 0.6 g/g.

average diameter of ∼12 nm and a density of ∼4 g/cm^3,[22] the surface area value of 80 m^2 g^{-1} can be obtained, which is consistent with our measurement. This further confirmed that all the nanowire within this sample are individual.

We have further found out that these in situ synthesized aerogels have superior mechanical properties, enabled by the long length of the nanowires in the network. Figure 2a shows the flexibility and bendability the cryptomelane nanowire aerogels made by the in situ synthesis, which can repeat many times without fracture. Also, the photographs in Figure 2b show that these nanowire aerogels can be compressed greatly but then restored completely when the pressure is released (for the testing here, a simple vapor deposition process[16] was carried out that produces a few nm organic coating on the nanowires inside the aerogel[16]). Figure 2c presents the result of the tension test. Four samples are measured here: B-96h-16 mg/cm^3 refers to the sample made with concentration B for 96 h synthesis, and the resulting density is 16 mg/cm^3; the other three samples use similar notation. From this data, it can be seen that first the Young's modulus (E) and tensile strength increase with aerogel density because higher density samples have more intertwining connections within the network and thus are stiffer and stronger. Second, both B-5h-10 mg/cm^3 and B-45h-10 mg/cm^3 have the same density, but B-45h-10 mg/cm^3 shows higher Young's modulus and tensile strength; this can be understood from the SEM image in Figure 1c,d. Sample B-5h-10 mg/cm^3 has the chestnut-bur-like structure; at each "island" the density of nanowires is high, but much fewer are long enough to connect to the neighboring islands. In contrast, for sample B-45h-10 mg/cm^3 the nanowires are evenly distributed in length and also appear to have longer length, which gives rise to higher stiffness and strength of the resulting aerogel. The ultimate tensile strength (UTS) for sample B-96h-16 mg/cm^3 is ∼1.1 MPa, which is remarkably higher than that of other porous materials, which is typically on the order of kPa.[23] Figure 2d shows the Young's modulus E versus sample density (ρ) for our aerogel samples compared with other aerogels reported previously.[13,23−30] It can be seen that at comparable density, our in situ aerogels shows much higher Young's modulus.[13,23−26] Especially for the 4 mg/cm^3 sample, it has a high E of 2.5 MPa, the highest compared to aerogels made of other materials at such low density. Considering the fact that our aerogels are built mainly via the van der Waals interaction between the nanowires, while the earlier reported ones are made via covalent bonding between the networks (for alumina, silica aerogels, or nanotube aerogels with carbon nanoparticles as a binder), the results here are striking. This suggests that the role played by the entanglement between the nanowires is significant, and apparently longer nanowires are much more favored. Indeed the cryptomelane nanowire aerogels made by our previous method[10] did not have such remarkable mechanical properties. The Young's modulus of the in situ aerogels increased with an increase in ρ with a power-law dependence of ∼2, similar to the Ni metallic lattice[26] and the graphene-based cellular monoliths,[24] in contrast to the $E \sim \rho^3$ scaling observed for ultralight aerogels and carbon nanotube foams with stochastic architecture.

The extraordinary mechanical properties can be also seen in the compression tests. Figure 2e shows that our aerogel with a

dx.doi.org/10.1021/nl404392j | Nano Lett. XXXX, XXX, XXX−XXX

low density of 4 mg/cm^3 (C-48h-4 mg/cm^3) could bear a compressive strain (ε) as high as 90%. Furthermore, this low-density aerogel shows superelastic behavior, that is, the aerogel was able to completely recover to its original shape when released from compression (Figure 2b and Supporting Information Movie S1). The compression tests with the other in situ aerogel samples were also carried out and the results are shown in Figure 2f. All the higher density samples also show elastic behavior at high compressive strains. As potential of aerogels for technological applications has often been limited by their poor mechanical properties, the superior mechanical properties obtained by the in situ synthesis method serve as an important advantage for their applications.

This general principle of gel formation during the hydrothermal synthesis can be applied to various nanowire hydrogel/aerogel syntheses. Figure 3a−c shows the SEM image of TiO_2 nanowire aerogels grown in situ with reaction times of 4 h (Figure 3a), 16 h (Figure 3b), and 48 h (Figure 3c). The TiO_2 nanowire growth follows similar pattern as the cryptomelane manganese oxide one, that is, the network shows chestnut-bur-like structure at shorter reaction times, and becomes much more uniform as time goes on. Furthermore, by tuning the precursor composition (i.e., whether KOH is used or NaOH is used), TiO_2 nanowires with either 5−10 nm diameter or 50−60 nm diameter can be synthesized (Figure 3d shows the SEM image of the TiO_2 nanowire aerogel with 50−60 nm diameter). Figure 3e−g shows the HRTEM and XRD characterizations of the TiO_2 nanowires; all the synthesis conditions produced high crystalline anatase TiO_2 nanowires. Figure 3h shows the BET surface area characterization of the sample in Figure 3b, a 292 m^2 g^{-1} surface area is obtained as the nanowires here have much smaller diameter. Because many different types of nanowires can be synthesized via the hydrothermal method, the method presented here is very powerful in producing various inorganic nanowire hydrogels and aerogels with tunable structure and properties.

A further advantage of our in situ synthesis method is that the nanowires in the hydrogels/aerogels serve both as structural scaffold for the bulk monolith and active functional sites on the nanoscale. Consider the two example systems explored in this work, manganese oxide and titanium oxide; both their nanoparticles and nanowires have been widely used for catalysis (or photocatalysis),[32] sensing,[6] energy storage[33] or conversion,[34] and so forth. However, in order to have a bulk form structure supports or scaffolds are needed, for example, TiO_2 nanoparticles have been deposited onto a metal grid to photocatalytically decompose organic pollutant in water.[35] However, the surface area of the resulting composite is much reduced and it is also a question whether the TiO_2 nanoparticles can adhere to the surface strong enough. Membranes with TiO_2 and MnO_2 nanowires have also been made[14,16] but also with reduced surface area and inferior mechanical properties (for example, the membranes made with cryptomelane nanowires by us previously[16] tend to break up when soaked in water). With these in situ grown nanowire aerogels, not only are large area active sites preserved, robust structural support is also provided at the same time. A particular example we explored here is to use these one-step synthesized hydrogels directly as water filters to remove toxic pollutants such as organic dyes and heavy metal ions. Compared to previously investigated materials for water filtration such as active carbon,[36] nanoclay,[37] graphene oxide,[38] or metal oxide nanoparticles,[39] no additional effort is needed for collecting or assembling the active material. The inset in Figure 4a shows the photograph of a syringe filter. An as-grown cryptomelane nanowire hydrogel is cut in shape and fit into the assembly (which cannot be seen in the photograph) so that when water solution containing methylene blue (MB) (the blue liquid in the syringe) passes through the filter and only clear water comes out (collected in the vial). Using UV−vis-spectrum (Figure 4a) it can be seen that MB was removed completely from the water. This excellent filtering effect is likely due to the high surface area of the hydrogel filter and electrostatic forces between the filter and the dye.[13] Furthermore, we investigated the performance of the nanowire hydrogels as water filters for the removal of heavy metal ions: 1000 ppm Pb^{2+}, 1000 ppm of Cd^{2+}, 100 ppm of $Cr_2O_7^{2-}$, or 100 ppm of Cu^{2+}. The nanowire hydrogel filters exhibited highly efficient performance to remove metal ions; with 1 mL volume of the solution, the initial uptake for Pb^{2+}, Cd^{2+}, $Cr_2O_7^{2-}$, or Cu^{2+} was found to be 100, 91, 95, or 88.3%, respectively, and the uptake only decreased to 78, 70, 75, 59%, respectively by 15 mL volume (Figure 4b). For these filtration tests, the uptake capability (here defined as the ratio of the removed metal ion amount to absorbent amount at 80% removal efficiency) is found to be Pb^{2+} > Cd^{2+} > $Cr_2O_7^{2-}$ > Cu^{2+}. In particular, the uptake capability 0.36 g/g for Pb^{2+} ions shows selectively higher efficiency than other metal ions, possibly due to the negative surface charge and the inherent tunnel structures of manganese oxide.[13] Also in Figure 4d, the absorption test using different absorbent dosages of 0.02, 0.04, 0.06, 0.08, and 0.1 g cryptomelane nanowire hydrogels shows exceptionally high removal of 47, 87.8, 100, 100, and 100%, respectively. The uptake capability from the absorption test (calculated from the slope of Figure 4d) is found to be 0.6 g/g, which is the highest absorption value, when compared with previous reported values.[36,37,40−43] As a result, it can be concluded that the porous cryptomelane nanowire hydrogel filters can be used very efficiently in the removal of heavy metal ions, especially lead ions from industrial wastewaters.

In conclusion, we developed a facile methodology to enable ultralight and highly porous inorganic nanowire hydrogels/aerogels production from in situ nanowire growth. The networks with interconnected inorganic nanowires were obtained by one-step hydrothermal synthesis without supporting materials. The density, porosity, and properties of the nanowire networks can be controlled by the initial concentration and reaction time. Superior properties such as high porosity and high surface allow these hydrogels/aerogels to be used in many areas, such as catalysis or photocatalysis, sensing, energy storage, and so forth. In this work, we investigated particularly the water filtration and found excellent performance from these one-step made water filters. As the nanowires act as both the skeleton for the bulk monolith and the active functional sites, the method is both simple and powerful. We anticipate that many more varieties of nanowire hydrogels/aerogels can be produced via this methodology for various different applications in the future.

Experimental Section. *Cryptomelane Manganese Oxide ($K_{2-x}Mn_8O_{16}$) Nanowire Hydrogel/Aerogels Production.* The starting materials were composed of 19.1 mmol of potassium sulfate (K_2SO_4), potassium persulfate ($K_2S_2O_8$), and manganese sulfate monohydrate ($MnSO_4{\cdot}H_2O$) in a ratio of 1:2:1 in 5 mL of DI water.[10,16] The precursor suspension was initially dispersed by ultrasonication at room temperature, and filtration and dilution was used to avoid undissolved precipitates (A,

dx.doi.org/10.1021/nl404392j | Nano Lett. XXXX, XXX, XXX−XXX

precursor suspensions without any treatment; B, filtration of A with a 0.8 μm syringe filter; C, 2-fold dilutions of B; D, 3-fold dilutions of the suspension after filtration of A with a 0.2 μm syringe filter). The suspensions were transferred to a Teflon vessel and the sealed vessel was heated in an oven at 523 K for 10 min to 96 h of reaction time. The in situ cryptomelane manganese oxide ($K_{2-x}Mn_8O_{16}$) nanowire hydrogels were washed with excess DI water and were cut into various shapes with a blade and then were placed into anhydrous ethanol overnight for solvent exchange. After that, the in situ nanowire hydrogels were supercritically dried into aerogels to retain the original gel volume.

Titanate Nanowire Aerogels Production. Commercially available P25 (anatase TiO_2 nanoparticles) was dissolved in 10 M KOH or NaOH solution and the concentration of P25 was 7.5 mg/mL. The mixture was stirred for 30 min and transferred to a Teflon vessel held in a stainless steel vessel. The sealed vessels were placed in an oven and heated at 453 or 523 K for 4 to 96 h, respectively. $K_2Ti_8O_{17}$ or $Na_2Ti_8O_{17}$ nanowire hydrogels were synthesized by a simple hydrothermal reaction of TiO_2 particles and KOH or NaOH solution and then ion-exchanged into $H_2Ti_8O_{17}$ by acid treatment (0.2 M HNO_3). After that, the hydrogels were washed with excess DI water without stirring or filtering to keep the gel networks intact and then were cut into various shapes with a blade and subsequently placed into anhydrous ethanol overnight for solvent exchange. After that, the in situ $H_2Ti_8O_{17}$ nanowire hydrogels were supercritically dried into aerogels to retain the original gel volume. Finally, $H_2Ti_8O_{17}$ nanowire hydrogels were transformed into anatase TiO_2 nanowire aerogels by calcination at 600 °C for 4 h.

■ ASSOCIATED CONTENT

Supporting Information

Additional figures for SEM images of cryptomelane and TiO_2 nanowire networks. The measurement of oil/solvent absorption and water filtration/absorption. This material is available free of charge via the Internet at http://pubs.acs.org.

■ AUTHOR INFORMATION

Corresponding Author

*E-mail: jingkong@mit.edu. Tel: +1-617-324-4068.

Author Contributions

⊥These authors contributed equally to this work.

Notes

The authors declare no competing financial interest.

■ ACKNOWLEDGMENTS

The authors gratefully acknowledge the funding from the MIT Energy Initiative, the National Science Foundation award number NSF DMR 0845358, and the generous gift from Doug Spreng. M.S.D. gratefully acknowledge NSF Grant DMR-100414. S.M.J acknowledges MIT Institute of Soldier Nanotechnologies (ISN) for the access of various instruments to carry out this work and the help from Professor Pablo Jarillo-Herrero, Dr. Su-Ryon Shin, and Dr. Tingying (Helen) Zeng.

■ REFERENCES

(1) Xu, S.; Qin, Y.; Xu, C.; Wei, Y.; Yang, R.; Wang, Z. L. *Nat. Nanotechnol.* **2010**, *5*, 366−373.

(2) Wang, D.; Luo, H.; Kou, R.; Gil, M. P.; Xiao, S.; Golub, V. O.; Yang, Z.; Brinker, C. J.; Lu, Y. *Angew. Chem., Int. Ed.* **2004**, *43* (45), 6169−6173.

(3) Wang, H.; Xu, C.; Cheng, F.; Jiang, S. *Electrochem. Commun.* **2007**, *9* (5), 1212−1216.

(4) Lee, J. M.; Choung, J. W.; Yi, J.; Lee, D. H.; Samal, M.; Yi, D. K.; Lee, C.; Yi, G.; Paik, U.; Rogers, J. A.; Park, W. I. *Nano Lett.* **2010**, *10* (8), 2783−2788.

(5) Rauber, M.; Alber, I.; Mller, S.; Neumann, R.; Picht, O.; Roth, C.; Schkel, A.; Toimil-Molares, M. E.; Ensinger, W. *Nano Lett.* **2011**, *11* (6), 2304−2310.

(6) Korhonen, J. T.; Hiekkataipale, P.; Malm, J.; Karppinen, M.; Ikkala, O.; Ras, R. H. A. *ACS Nano* **2011**, *5*, 1967−1974.

(7) Li, F.; Yao, X.; Wang, Z.; Xing, W.; Jin, W.; Huang, J.; Wang, Y. *Nano Lett.* **2012**, *12*, 5033−5038.

(8) McGrath, K. M.; Dabbs, D. M.; Yao, N.; Aksay, I. A.; Gruner, S. M. *Science* **1997**, *277*, 552−556.

(9) Tokarev, I.; Minko, S. *Adv. Mater.* **2010**, *22*, 3446−3462.

(10) Jung, S. M.; Jung, H. Y.; Dresselhaus, M. S.; Jung, Y. J.; Kong, J. *Sci. Rep.* **2012**, *2*, 849.

(11) Wang, X.; Li, Y. *J. Am. Chem. Soc.* **2002**, *124* (12), 2880−2881.

(12) Pavasupreea, S.; Suzukia, Y.; Yoshikawaa, S.; Kawahata, R. *J. Solid State Chem.* **2005**, *178*, 3110−3116.

(13) Long, Y.; Hui, J.-F.; Wang, P.-P.; Hu, S.; Xu, B.; Xiang, G.-L.; Zhuang, J.; Lu, X.-Q.; Wang, X. *Chem. Commun.* **2012**, *48*, 5925−5927.

(14) Hu, A.; Zhang, X.; Oakes, K. D.; Peng, P.; Zhou, Y. N.; Servos, M. R. *J. Hazard. Mater.* **2011**, *189*, 278−285.

(15) Xia, Y.; Yang, P.; Sun, Y.; Wu, Y.; Mayers, B. G.; Yin, Y.; Kim, F.; Yan, H. *Adv. Mater.* **2003**, *15*, 353−389.

(16) Yuan, J.; Liu, X.; Akbulut, O.; Hu, J.; Suib, S. L.; kong, J.; Stellacci, F. *Nat. Nanotechnol.* **2008**, *3*, 332−336.

(17) Suib, S. L.; Yuan, J. U.S. Pat. Appl. Publ. U.S.2006049101, 2006.

(18) Yuan, J.; Laubernds, K.; Villegas, J.; Gomez, S.; Suib, S. L. *Adv. Mater.* **2004**, *16*, 1729−1732.

(19) Xiwang, Z.; Tong, Z.; Jiawei, N.; Darren, D. S. *Adv. Funct. Mater.* **2009**, *19*, 3731−3736.

(20) Tian, Z. R.; Voigt, J. A.; Liu, J.; Mckenzie, B.; Xu, H. *J. Am. Chem. Soc.* **2003**, *125*, 12384.

(21) Zhang, Y. X.; Li, G. H.; Jin, Y. X.; Zhang, Y.; Zhang, J.; Zhang, L. D. *Chem. Phys. Lett.* **2002**, *365*, 300−304.

(22) Perez, H.; Navarro, P.; Torres, G.; Sanz, O.; Montes, M. *Catal. Today* **2013**, *212*, 149−156.

(23) Mecklenburg, M.; Schuchardt, A.; Mishra, Y. K.; Kaps, S.; Adelung, R.; Lotnyk, A.; Kienle, L.; Schulte, K. *Adv. Mater.* **2012**, *24*, 3486−3490.

(24) Qiu, L.; Liu, J. Z.; Chang, S. L.Y.; Wu, Y.; Li, D. *Nat. Commun.* **2012**, *3*, 1241.

(25) Kim, K. K.; Oh, Y.; Islam, M. F. *Adv. Funct. Mater.* **2013**, *23*, 377−383.

(26) Schaedler, T. A.; Jacobsen, A. J.; Torrents, A.; Sorensen, A. E.; Lian, J.; Greer, J. R.; Valdevit, L.; Carter, W. B. *Science* **2011**, *334*, 962−965.

(27) Zhang, X.; Sui, Z.; Xu, B.; Yue, S.; Luo, Y.; Zhan, W.; Liu, B.; Wanchu Zhan, B. L. *J. Mater. Chem.* **2011**, *21*, 6494−6497.

(28) Parmenter, K. E.; Milstein, F. *J. Non-Cryst. Solids* **1998**, *223*, 179−189.

(29) Guo, H.; Meador, M. A. B.; McCorkle, L.; Quade, D. J.; Guo, J.; Hamilton, B.; Cakmak, M. *ACS Appl. Mater. Interfaces* **2012**, *4*, 5422−5429.

(30) Andrews, E.; Sanders, W.; Gibson, L. J. *Mater. Sci. Eng., A* **1999**, *270*, 113−124.

(31) Yuan, J. *Colloids Surf., A* **2004**, *241*, 173−183.

(32) Zhang, X.; Zhang, T.; Ng, J.; Sun, D. D. *Adv. Funct. Mater.* **2009**, *19*, 3731−3736.

(33) Li, W.; Liu, Q.; Sun, Y.; Sun, J.; Zou, R.; Li, G. X.; Song, G.; Ma, G.; Yang, J.; Chen, Z.; Junqing, H. *J. Mater. Chem.* **2012**, *22*, 14864−14867.

(34) Xu, M.; Da, P.; Wu, H.; Zhao, D.; Zheng, G. *Nano Lett.* **2012**, *12* (3), 1503−1508.

(35) Li, W.; Shah, S. I.; Sung, M.; Hung, C. P. *J. Vac. Sci. Technol., B* **2002**, *20* (6), 2303−2308.
(36) Acharya, J.; Sahu, J. N.; Mohanty, C. R.; Meikap, B. C. *Chem. Eng. J.* **2009**, *149*, 249−262.
(37) Lagadic, I. L.; Mitchell, M. K.; Payne, B. D. *Environ. Sci. Technol.* **2001**, *35*, 984−990.
(38) Gao, W.; Majumder, M.; Alemany, L. B.; Narayanan, T. N.; Ibarra, M. A.; Pradhan, B. K.; Ajayan, P. M. *ACS Appl. Mater. Interfaces* **2011**, *3*, 1821−1826.
(39) Chen, H.; He, J. *J. Phys. Chem. C* **2008**, *112*, 17540−17545.
(40) Oscar, H. R.; Stuart, M. H. *J. Mater. Chem.* **2008**, *18*, 2751−2761.
(41) Karami, H. *Chem. Eng. J.* **2013**, *219*, 209−216.
(42) Huang, Z.; Wu, Q.; Liu, S.; Liu, T.; Zhang, B. *Carbohydr. Polym.* **2013**, *97* (2), 496−501.
(43) Maryam, A. T.; Toraj, M. *J. Hazard. Mater.* **2011**, *185*, 140−147.

dx.doi.org/10.1021/nl404392j | *Nano Lett.* XXXX, XXX, XXX−XXX